

Optimizing Vehicle Ride Comfort using GA-LQR Control in In-Wheel Suspension Systems

A Generation System for Autonomous Vehicle

Do Trong Tu

Faculty of Mechanical - Automotive and Civil Engineering, Electric Power University, Hanoi, Vietnam
tudt@epu.edu.vn (corresponding author)

Received: 21 November 2024 | Revised: 6 January 2025 | Accepted: 24 January 2025

Licensed under a CC-BY 4.0 license | Copyright (c) by the authors | DOI: <https://doi.org/10.48084/etasr.9684>

ABSTRACT

Controlled suspension systems, particularly active in-wheel suspension systems, are increasingly adopted in electric and autonomous vehicles due to their compact design and adaptability to various operating conditions. This study proposes the implementation of Linear Quadratic Regulator (LQR) controllers to improve vehicle smoothness and safety criteria. Genetic Algorithms (GA) are employed to optimize the weighting parameter values in the objective function in LQR controller, which allow them to adapt to the vehicle's condition. The simulation results demonstrate that the proposed controller model enhances system performance by up to 14% in comparison with conventional models. These findings suggest that the proposed system significantly enhances the feasibility of meeting user requirements in modern vehicle applications.

Keywords-active inwheel suspension; genetic algorithm optimization; vehicle vibration; vehicle dynamic; ride quality

I. INTRODUCTION

The automotive industry is undergoing a transformative shift due to the rapid advancements in autonomous vehicle technology. This shift promises enhanced safety, efficiency, and accessibility. At the core of this transformation is the development of sophisticated systems that ensure safe and reliable operation while prioritizing passenger comfort and vehicle performance [1, 2]. Conventional suspension systems, while demonstrating effectiveness, encounter challenges in rapidly adapting to the fluctuating road conditions and dynamics. To address these challenges, researchers are exploring active in-wheel suspension systems, which offer innovative solutions to meet the evolving demands of autonomous vehicles [3, 4]. These systems integrate advanced control mechanisms and in-wheel motors, enabling precise, independent wheel control, thereby optimizing ride comfort, stability, and performance in real time. Although these systems enhance handling, traction, and weight distribution, the augmented unsprung mass introduces complexities necessitating a meticulous examination of the suspension dynamics. To this end, the present study employs the quarter-car model, which has gained a reputation for its simplicity and effectiveness in capturing vertical vehicle dynamics, to assess the impact of in-wheel motors on suspension performance [5, 6]. This model incorporates the primary suspension components, such as the main spring and damper, as well as the secondary suspension elements specific to the in-wheel motor, including a spring and damper. Additionally, the integration of an active force actuator is contemplated to examine the

prospect of augmenting ride comfort and handling [7-9]. The integration of in-wheel motors into vehicle systems signifies a substantial advancement in the realm of automotive engineering. This integration offers several advantages, including improved weight distribution, enhanced vehicle handling, and the potential for advanced traction control. However, this integration introduces challenges, particularly concerning the dynamics of the suspension system due to increased unsprung mass. This literature review aims to provide a comprehensive examination of the extant research and contributions to the field of active in-wheel suspension systems. It does so by highlighting advancements and identifying research gaps. Authors in [10-13] provide foundational insights into vehicle dynamics and the role of suspension systems in achieving ride comfort and stability. The fuzzy active suspension system, designed in [14], aims to balance performance and complexity through adaptive damping. The potential of in-wheel motors in electric vehicles has been extensively discussed, addressing efficiency, control strategies, and integration challenges [13].

Authors in [15] explore the repercussions of augmented unsprung mass on vehicle dynamics and put forward modifications to ameliorate deleterious effects. Authors in [16] focus on the dynamic behavior of electric vehicles equipped with in-wheel motors, underscoring the merits and limitations of four-wheel independent drive systems. Authors in [17] propose an advanced suspension model integrating in-wheel motors, emphasizing adaptive GPSO-LQG control strategies. Authors in [18] optimize suspension systems for vehicles with in-wheel motors, stressing tailored designs by GA such that

significant handling and comfort improvements are achieved in an electric vehicle prototype. Authors in [19] present a dynamic model highlighting integrated control strategies, while authors in [20] propose a new active suspension design for electric vehicles, focusing on ride quality and stability. These studies underscore the potential of active in-wheel suspension systems to transform vehicle dynamics and enhance the overall performance of autonomous and (or) electric vehicles. Authors in [21] used an optimal switching controller with a magnetorheological damper and road type classification to apply appropriate control inputs for improved ride and stability, as demonstrated through computer simulations. This study aims to address a significant gap in the current literature by developing a detailed quarter-car model that incorporates the mass of the in-wheel motor and its associated suspension components. This model is expected to facilitate a more profound comprehension of the dynamic behavior of vehicles equipped with in-wheel motors and to optimize suspension systems for enhanced performance.

II. MATERIALS AND METHODS

A. Vehicle Model with Active in-Wheel Suspension

As presented in Figure 1 and Table I, the design concepts and physical characteristics of a quarter-car suspension system featuring an in-wheel suspension system are delineated. It is important to note that the absorber is excluded and the in-wheel motor is directly attached to the wheel. As a result, the active suspension forms a new automotive topological structure, specifically an active suspension with a centralized in-wheel motor [7].

TABLE I. THE PARAMETERS OF THE QUARTER VEHICLE

Abbreviation	Description	Value	Unit
m_s	Sprung mass	275	kg
m_u	Wheel mass	35	kg
m_m	Motor mass	32	kg
k_s	Suspension stiffness	22,000	N/m
c_s	Suspension damping coefficient	200	Ns/m
k_m	Stiffness of damper for motor	15,000	N/m
c_m	Damping coefficient for motor	150	Ns/m
k_u	Tire stiffness	200,000	N/m

The development of the proposed model may be formulated as:

$$m_s \ddot{Z}_s = -k_s(Z_s - Z_u) - c_s(\dot{Z}_s - \dot{Z}_u) + F \quad (1)$$

$$m_u \ddot{Z}_u = k_s(Z_s - Z_u) + c_s(\dot{Z}_s - \dot{Z}_u) + k_m(Z_m - Z_u) + c_m(\dot{Z}_m - \dot{Z}_u) - k_u(Z_u - Z_r) - F \quad (2)$$

$$m_m \ddot{Z}_m = -k_m(Z_m - Z_u) - c_m(\dot{Z}_m - \dot{Z}_u) \quad (3)$$

where Z_s , Z_u , Z_m are the vertical displacement of sprung mass, unsprung mass, and motor, respectively, while Z_r is the road disturbance.

B. The Actuator in the Active In-Wheel Suspension Model

The Bouc-Wen model plays a critical role in the analysis of hysteresis behavior in dampers within active suspension systems. It effectively captures the complex, non-linear, and path-dependent nature of damping forces. The integration of

this model enables engineers to simulate and control the dynamic behavior of active suspensions with greater precision. The model's differential equations embody the hysteretic behavior, thus facilitating the design of adaptive control algorithms that dynamically adjust suspension forces to optimize ride comfort and handling [22]. Recent research has focused on enhancing the Bouc-Wen model's accuracy and performance, including the integration of neural networks and GA for real-time adaptation and parameter optimization [23]. The Bouc-Wen model is a phenomenological model that represents the hysteresis behavior through a set of differential equations. The model has proven to be particularly effective in capturing the energy dissipation and restoring force characteristics of dampers, thus making it a popular choice for modeling semi-active and active suspension systems, as shown in Figure 2. The general form of the Bouc-Wen model for hysteresis can be described as:

$$F = c_o(\dot{Z}_s - \dot{Z}_u) + k_o(x - x_o) + \alpha z \quad (4)$$

$$\dot{z} = -\gamma|\dot{Z}_s - \dot{Z}_u|z|z|^{n-1} - \beta\dot{x}|z|^n + \alpha\dot{x} \quad (5)$$

where z is the hysteretic displacement, F is the restoring force, α , β , γ , are parameters that shape the hysteresis loop.

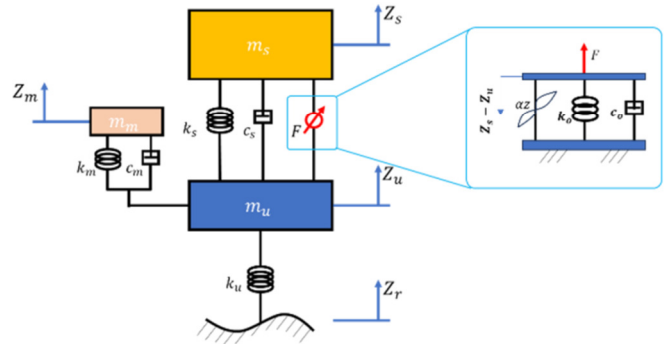


Fig. 1. The quarter vehicle with in wheel suspension system.

C. Design Linear Quadratic Regulator and Genetic Algorithm Controllers for Active In-Wheel Suspension Model

According to the principles of the control theory, the differential equation of the active suspension system is transformed into a state-space metric:

$$\begin{cases} \dot{x} = Ax + B_1u + B_2w \\ y = Cx + D_1u + D_2w \end{cases} \quad (6)$$

In order to develop a comprehensive understanding of the system's behavior, it is essential to consider the state vector in relation to the movement of the suspension system, the velocity of the sprung mass, the displacement of the tire relative to the road, the rapidity of the unsprung mass, the dislocation of the motor in comparison to the unsprung mass, and the velocity of the in-wheel motor:

$$x = [Z_s - Z_u \quad \dot{Z}_s \quad Z_u - Z_r \quad \dot{Z}_u \quad Z_m - Z_u \quad \dot{Z}_m]^T \quad (7)$$

The control and disturbance vectors are defined as the damper force and the displacement from the road, respectively:

$$w = Z_r, u = F \quad (8)$$

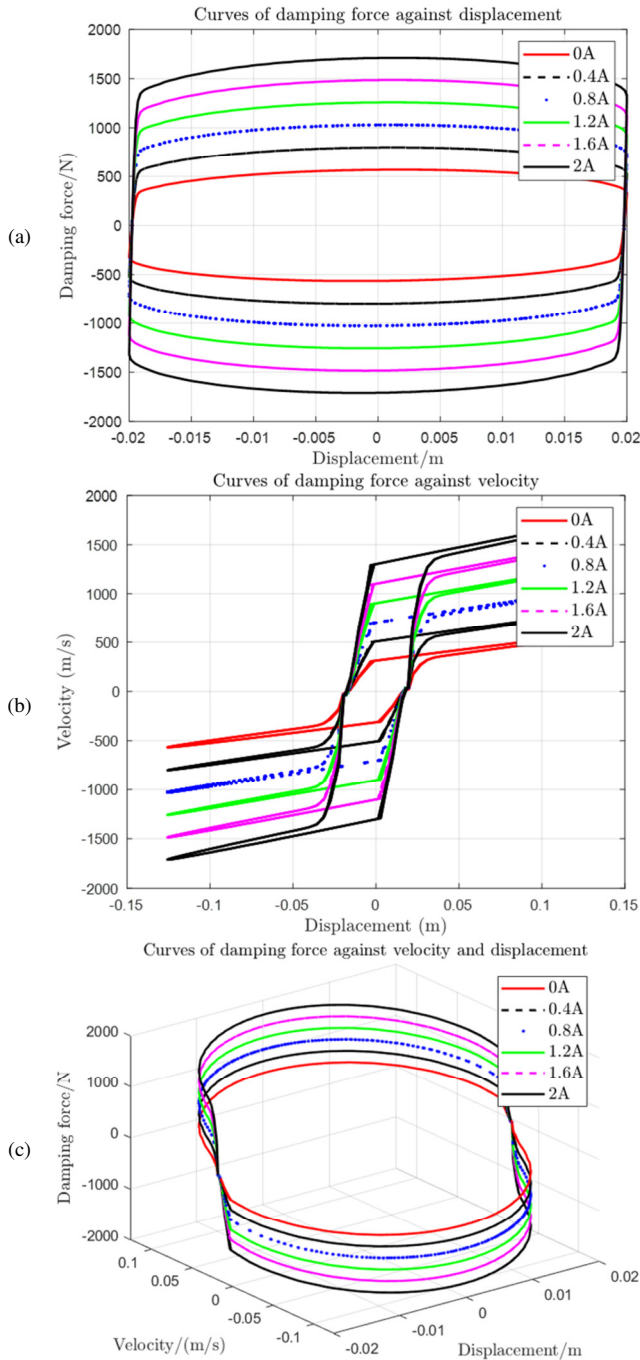


Fig. 2. The relationship in the Bouc-Wen actuator: (a) damping force and displacement, (b) damping force and velocity, (c) damping force, displacement and velocity due to the varying current.

The measured output vector is:

$$y = [Z_s - Z_u \quad \dot{Z}_s \quad Z_u - Z_r \quad \dot{Z}_u \quad Z_m - Z_u \quad \dot{Z}_m]^T \quad (9)$$

The objective of the control task is to identify factors that facilitate the rapid recovery of the state variable vector to a predicted state in the event of an unrecognized external impact on the road. That is to say, external factors must be rapidly suppressed to prevent oscillations. The use of multiple control

approaches can ensure the mitigation of these problems. To enhance the vehicle's overall dynamic performance, it is imperative to consider all assessment indications while constructing the LQR controller. In accordance with these considerations, the present study delineates the comprehensive objective performance J as:

$$\min J = \lim_{T \rightarrow \infty} \frac{1}{T} E \left[\int_0^T (x^T Q x + u^T R u) dt \right] \quad (10)$$

With the output vector in (9) the objective performance in (10) is now equivalent to:

$$J = \int_0^T \left[\rho_1 (Z_s - Z_u)^2 + \rho_2 (\dot{Z}_s)^2 + \rho_3 (Z_u - Z_r)^2 + \rho_4 (\dot{Z}_u)^2 + \rho_5 (Z_m - Z_u)^2 + \rho_6 (\dot{Z}_m)^2 \right] \quad (11)$$

$$f = \delta rms(\dot{Z}_s) + (1 - \delta) rms(\dot{Z}_u) \quad , \delta = [0 \div 1] \quad (12)$$

$$\begin{cases} rms(\dot{Z}_s) \leq 1.6 (m/s^2) \\ rms(\dot{Z}_u) \leq 0.8 (m/s^2) \\ rms(\dot{Z}_m) \leq 0.2 (m/s^2) \\ rms(Z_u - Z_r) \ll 0 (m) \end{cases} \quad (13)$$

According to the aforementioned assertions, the efficacy of an LQR controller is contingent upon the judicious selection of weighting parameters, namely $\rho_1, \rho_2, \rho_3, \rho_4, \rho_5, \rho_6$, which can prove complicated to calibrate manually. To circumvent this challenge, the employment of GAs, drawing parallels with natural selection, enables the automation of the optimization process, thereby facilitating the identification of optimal weighting parameters. The GA iteratively evolves a population of 50 candidate solutions, evaluating the performance of f in (12), using a fitness function in (13) derived from the LQR cost function in (11). Through selection, crossover, and mutation, the GA refines the population, converging towards an optimal set of weighting parameters that enhance the controller's performance, as depicted in Table II. This approach not only simplifies the tuning process, but also ensures a more robust and efficient LQR controller design.

TABLE II. THE WEIGHTING PARAMETERS FOR LQR CONTROLLERS BY GA

Controller	ρ_1	ρ_2	ρ_3	ρ_4	ρ_5	ρ_6
Initial LQR	90,000	50,000	10,000	8,000	20,000	50,000
LQR+GA1 ($\delta = 0.1$)	87,501	69,969	58,016	47,339	20,327	71,883
LQR+GA2 ($\delta = 0.5$)	46,277	49,195	43,283	49,821	46,977	49,066
LQR+GA3 ($\delta = 0.9$)	24,261	19,937	48,878	49,998	76,520	47,316

III. RESULTS AND DISCUSSION

The ISO 8608 standard is the benchmark for the classification of road roughness, using the Power Spectral Density (PSD) of the road profile to assess its quality. In this study, a Class C Road, characterized by its moderate roughness, is utilized as a reference. This road possesses a reference PSD value of $512 \times 10^{-6} \text{ m}^2/\text{cycle/m}$ at a spatial frequency of 0.1 cycles/m. To assess the proposed models, the spatial frequency is converted to temporal frequency based on a vehicle speed of 50 km/h, enabling a detailed evaluation of the road impact on vehicle dynamics in the time domain. Figures 3, 4 and 5 illustrate the vertical acceleration, velocity, and

displacement of the sprung and unsprung masses over time for various control strategies.

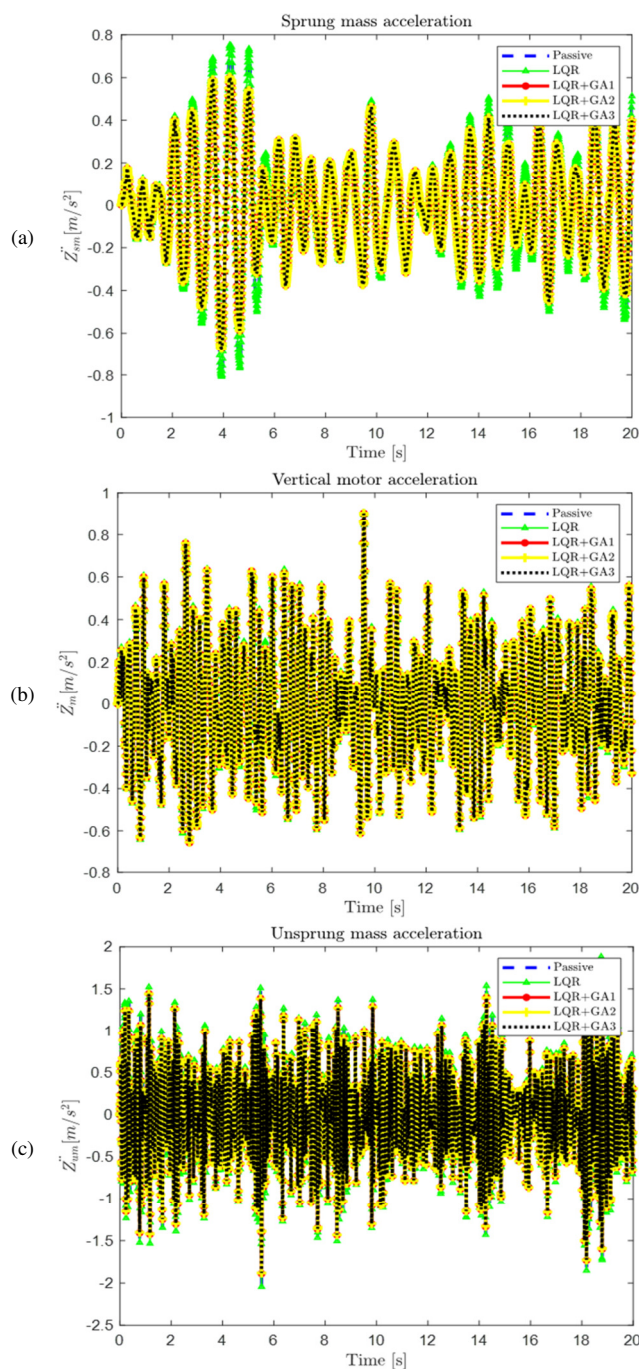


Fig. 3. The time response of: (a) acceleration of sprung mass, (b) acceleration of unsprung mass, (c) acceleration of in-wheel motor.

These include the passive model, depicted by a blue dashed line, the LQR controller, represented by a green line and triangle markers, LQR+GA1, displayed by a red line and circle markers, LQR+GA2, shown by a yellow line and plus markers, and LQR+GA3, which is represented by a black dashed line.

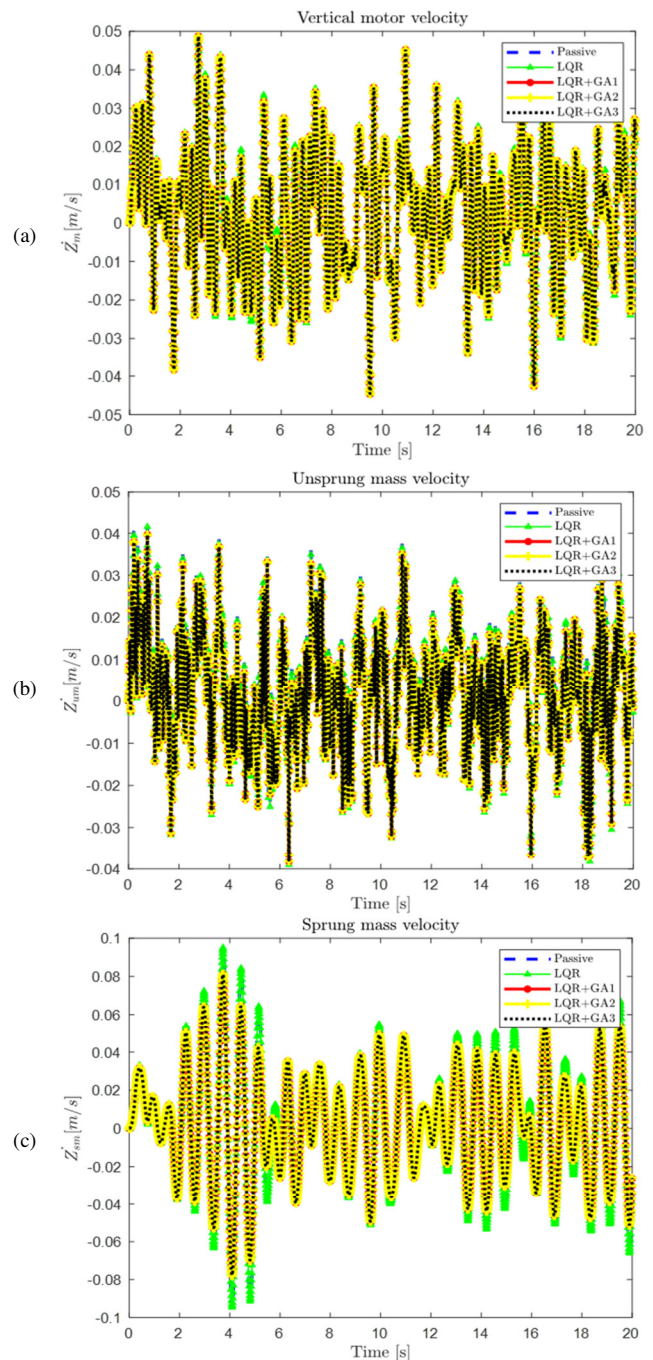


Fig. 4. The time response of: (a) velocity of sprung mass, (b) velocity of unsprung mass, (c) velocity of in-wheel motor.

As presented in Figure 3, the vertical accelerations of the sprung mass, unsprung mass, and in-wheel motor are observed under various control strategies. The passive system demonstrates substantial high-frequency oscillations across all cases, while LQR control mitigates these oscillations, enhancing stability and vibration damping. The incorporation of GA (LQR+GA1, GA2, GA3) further enhances performance, with LQR+GA3 demonstrating superiority in reducing sprung mass oscillations, LQR+GA2 achieving optimal performance

for the unsprung mass, and LQR+GA1 achieving the most consistent improvement for the in-wheel motor.

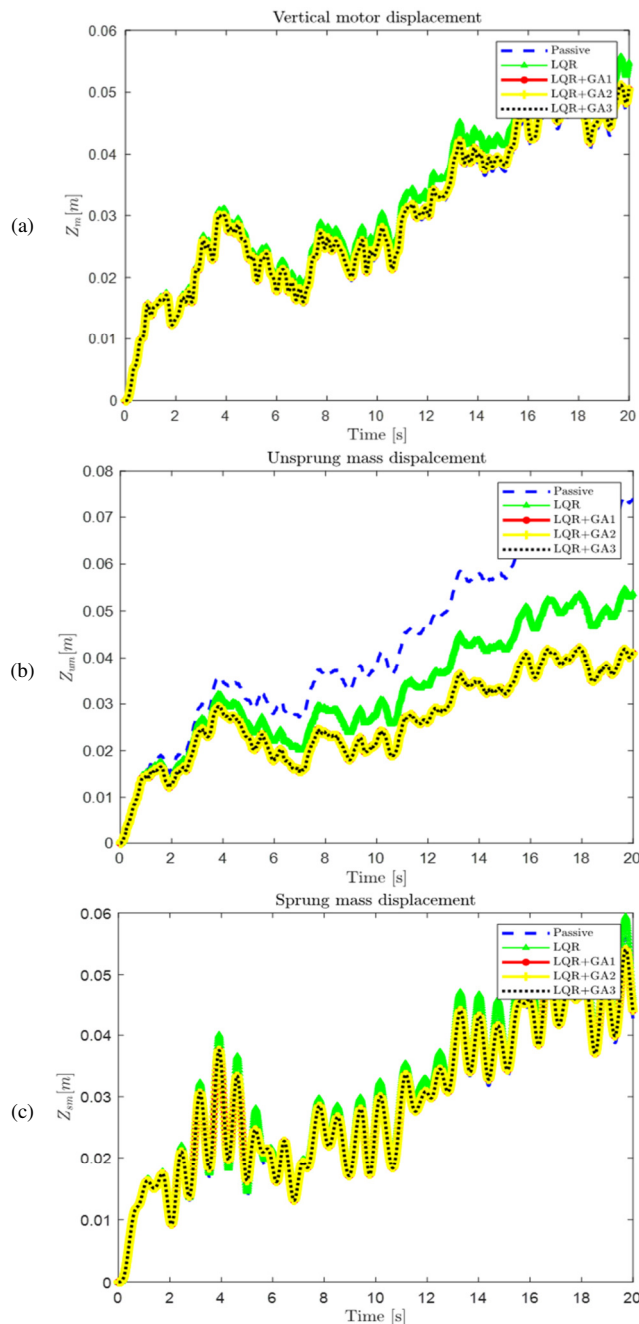


Fig. 5. The time response of: (a) displacement of sprung mass, (b) displacement of unsprung mass, (c) displacement of in-wheel motor.

A comparison of the proposed controllers with the uncontrolled system reveals a substantial enhancement in the velocity of the sprung mass in models GA1, GA2, and GA3, with reductions of 14.04%, 13.88%, and 14.02%, respectively. Concurrently, the velocity of the unsprung mass experiences a decline of approximately 2%, accompanied by a substantial reduction in displacement of more than 49%. In comparison

with a passive suspension system, the LQR controller has been shown to reduce the velocity of the sprung mass by up to 13.61%, with its velocity reduced by 9.93%. Furthermore, for the in-wheel motor, there are reductions in velocity and displacement of 2.33% and 10.65%, respectively, while the velocity and displacement of the unsprung mass in the proposed models decrease by 2.33% and 27.84%, respectively. These improvements underscore the efficacy of the proposed controllers in enhancing system performance. The substantial reductions in velocity and displacement for both the sprung and unsprung masses, as well as for the in-wheel motor, signify a considerable enhancement in stability and overall ride comfort.

As shown in Figure 6, the Bouc-Wen actuator generates control forces within the active in-wheel suspension system. In the passive system, the control force is zero. When using the LQR controller, the required control force for the system is minimal, less than 10N. However, when LQR controllers employing GA algorithms are used, the requisite control force escalates to approximately seven times greater magnitude. For instance, the LQR+GA1 model demands a force of up to 146N after four seconds.

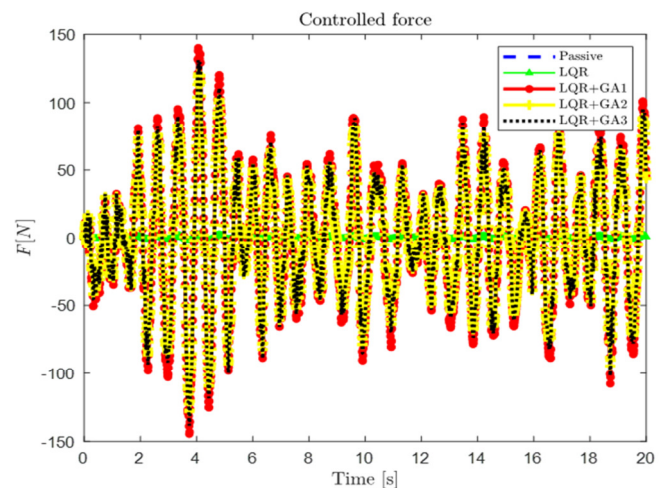


Fig. 6. The time response of force at the Bouc-Wen actuator.

In Table III presents a comparative analysis of the performance of LQR+GA1, LQR+GA2, and LQR+GA3 against passive and LQR systems with regard to acceleration, velocity, and displacement. It is evident that LQR+GA2 and LQR+GA3 demonstrate a modest enhancement in sprung mass acceleration, while LQR+GA1 exhibits a pronounced capability in reducing unsprung and middle mass acceleration. With respect to velocity, LQR+GA2 and LQR+GA3 have been observed to reduce sprung mass values, while LQR+GA1 has been shown to enhance unsprung and middle mass velocities. The differences in displacement are negligible, with LQR+GA2 exhibiting a marginal improvement in sprung mass displacement.

TABLE III. COMPARING THE REDUCTION OF REFERRED SIGNALS

	Signal	LQR+GA1	LQR+GA2	LQR+GA3
Passive	\ddot{Z}_s	14.90	14.72	14.87
	\ddot{Z}_u	6.32	6.65	6.67
	\ddot{Z}_m	0.19	0.52	0.50
	\dot{Z}_s	14.04	13.88	14.02
	\dot{Z}_u	1.94	2.02	2.02
	\dot{Z}_m	0.13	0.28	0.28
	Z_s	2.73	2.71	2.73
	Z_u	49.14	49.13	49.13
	Z_m	2.25	2.29	2.29
LQR	\ddot{Z}_s	14.50	14.32	14.47
	\ddot{Z}_u	6.83	7.16	7.18
	\ddot{Z}_m	0.01	0.34	0.32
	\dot{Z}_s	13.61	13.46	13.59
	\dot{Z}_u	2.25	2.32	2.33
	\dot{Z}_m	0.14	0.30	0.29
	Z_s	9.93	9.91	9.92
	Z_u	27.84	27.83	27.83
	Z_m	10.65	10.62	10.62

IV. CONCLUSIONS

The present study demonstrates the efficacy of Genetic Algorithm (GA)-optimized Linear Quadratic Regulator (LQR) controllers for active in-wheel suspension systems in electric and autonomous vehicles. The approach enhances smoothness and safety, reducing vehicle body acceleration by 15% compared to passive systems, and achieving a 14.50% improvement over traditional LQR models. These findings underscore the potential of GA-optimized controllers to satisfy contemporary vehicle requirements and enhance suspension system adaptability.

ACKNOWLEDGEMENT

The author sincerely thanks Electric Power University for their invaluable support and assistance, which greatly contributed to the study's success.

REFERENCES

- [1] C. Hecht, K. G. Spreuer, J. Figgenger, and D. U. Sauer, "Market Review and Technical Properties of Electric Vehicles in Germany," *Vehicles*, vol. 4, no. 4, pp. 903–916, Dec. 2022, <https://doi.org/10.3390/vehicles4040049>.
- [2] E. Yildirim and I. Esen, "Dynamic Behavior and Force Analysis of the Full Vehicle Model using Newmark Average Acceleration Method," *Engineering, Technology & Applied Science Research*, vol. 10, no. 1, pp. 5330–5339, Feb. 2020, <https://doi.org/10.48084/etasr.3335>.
- [3] Z. Zhao, H. Taghavifar, H. Du, Y. Qin, M. Dong, and L. Gu, "In-Wheel Motor Vibration Control for Distributed-Driven Electric Vehicles: A Review," *IEEE Transactions on Transportation Electrification*, vol. 7, no. 4, pp. 2864–2880, Dec. 2021, <https://doi.org/10.1109/TTE.2021.3074970>.
- [4] D. T. Tu, "Enhancing Road Holding and Vehicle Comfort for an Active Suspension System utilizing Model Predictive Control and Deep Learning," *Engineering, Technology & Applied Science Research*, vol. 14, no. 1, pp. 12931–12936, Feb. 2024, <https://doi.org/10.48084/etasr.6582>.
- [5] G. Long, F. Ding, N. Zhang, J. Zhang, and A. Qin, "Regenerative active suspension system with residual energy for in-wheel motor driven electric vehicle," *Applied Energy*, vol. 260, Feb. 2020, Art. no. 114180, <https://doi.org/10.1016/j.apenergy.2019.114180>.
- [6] M. Yu, S. A. Evangelou, and D. Dini, "Advances in Active Suspension Systems for Road Vehicles," *Engineering*, vol. 33, pp. 160–177, Feb. 2024, <https://doi.org/10.1016/j.eng.2023.06.014>.
- [7] D. T. Tu, "Active in-Wheel Suspension Performance Analysis Using Linear Quadratic Controllers," in *2023 International Conference on Control, Robotics and Informatics (ICCRI)*, Danang, Vietnam, May 2023, pp. 1–6, <https://doi.org/10.1109/ICCRI58865.2023.00008>.
- [8] S. Babesse, "Design of Two Optimized Controllers of a Hydraulic Actuator Semi-Active Suspension: A Comparison Study," *Engineering, Technology & Applied Science Research*, vol. 9, no. 4, pp. 4561–4565, Aug. 2019, <https://doi.org/10.48084/etasr.2836>.
- [9] R. N. Yerrawar and R. R. Arakerimath, "Parametric Analysis of Magnetorheological Strut for Semiactive Suspension System Using Taguchi Method," *Engineering, Technology & Applied Science Research*, vol. 8, no. 4, pp. 3218–3222, Aug. 2018, <https://doi.org/10.48084/etasr.2139>.
- [10] L. Zhang, S. Zhang, and W. Zhang, "Multi-objective optimization design of in-wheel motors drive electric vehicle suspensions for improving handling stability," *Proceedings of the Institution of Mechanical Engineers, Part D: Journal of Automobile Engineering*, vol. 233, no. 8, pp. 2232–2245, Jul. 2019, <https://doi.org/10.1177/0954407018783145>.
- [11] Z. Li, L. Zheng, Y. Ren, Y. Li, and Z. Xiong, "Multi-objective optimization of active suspension system in electric vehicle with In-Wheel-Motor against the negative electromechanical coupling effects," *Mechanical Systems and Signal Processing*, vol. 116, pp. 545–565, Feb. 2019, <https://doi.org/10.1016/j.ymssp.2018.07.001>.
- [12] T. Feng and L. Shu, "Game-Based Multiobjective Optimization of Suspension System for In-Wheel Motor Drive Electric Vehicle," *Mathematical Problems in Engineering*, vol. 2021, no. 1, 2021, Art. no. 5589199, <https://doi.org/10.1155/2021/5589199>.
- [13] Y. Qin, Z. Wang, K. Yuan, and Y. Zhang, "Comprehensive Analysis and Optimization of Dynamic Vibration-Absorbing Structures for Electric Vehicles Driven by In-Wheel Motors," *Automotive Innovation*, vol. 2, no. 4, pp. 254–262, Dec. 2019, <https://doi.org/10.1007/s42154-019-00079-9>.
- [14] A. A. Ahmed, H. A. Eissa, A. M. Faraj, A. Albagul, M. Belrzaeg, and A. Alsharif, "Suspension System Modelling And Control For An Electric Vehicle Driven by In-Wheel Motors," in *2021 IEEE International Conference on Robotics, Automation, Artificial-Intelligence and Internet-of-Things (RAAICON)*, Dhaka, Bangladesh, Dec. 2021, pp. 1–5, <https://doi.org/10.1109/RAAICON54709.2021.9929611>.
- [15] M. Liu, F. Gu, J. Huang, C. Wang, and M. Cao, "Integration Design and Optimization Control of a Dynamic Vibration Absorber for Electric Wheels with In-Wheel Motor," *Energies*, vol. 10, no. 12, Dec. 2017, Art. no. 2069, <https://doi.org/10.3390/en10122069>.
- [16] M. Liu, Y. Zhang, J. Huang, and C. Zhang, "Optimization control for dynamic vibration absorbers and active suspensions of in-wheel-motor-driven electric vehicles," *Proceedings of the Institution of Mechanical Engineers, Part D: Journal of Automobile Engineering*, vol. 234, no. 9, pp. 2377–2392, Aug. 2020, <https://doi.org/10.1177/0954407020908667>.
- [17] F. Ma, J. Wang, Y. Wang, and L. Yang, "Optimization design of semi-active controller for in-wheel motors suspension," *Journal of Vibroengineering*, vol. 20, no. 8, pp. 2908–2924, Dec. 2018, <https://doi.org/10.21595/jve.2018.19423>.
- [18] Z. Yang, C. Yong, Z. Li, and Y. Kangsheng, "Simulation analysis and optimization of ride quality of in-wheel motor electric vehicle," *Advances in Mechanical Engineering*, vol. 10, no. 5, May 2018, Art. no. 1687814018776543, <https://doi.org/10.1177/1687814018776543>.
- [19] M. Liu, F. Gu, and Y. Zhang, "Ride Comfort Optimization of In-Wheel-Motor Electric Vehicles with In-Wheel Vibration Absorbers," *Energies*, vol. 10, no. 10, Oct. 2017, Art. no. 1647, <https://doi.org/10.3390/en10101647>.
- [20] X. Shao, F. Naghdy, and H. Du, "Reliable fuzzy H_∞ control for active suspension of in-wheel motor driven electric vehicles with dynamic damping," *Mechanical Systems and Signal Processing*, vol. 87, pp. 365–383, Mar. 2017, <https://doi.org/10.1016/j.ymssp.2016.10.032>.
- [21] D.-S. Yoon and S.-B. Choi, "Adaptive Control for Suspension System of In-Wheel Motor Vehicle with Magnetorheological Damper," *Machines*,

- vol. 12, no. 7, Jul. 2024, Art. no. 433, <https://doi.org/10.3390/machines12070433>.
- [22] J. Zhao, M. Cui, R. Xu, Y. Li, F. Zhang, and Y. Cao, "High-Precision Position Tracking Control with a Hysteresis Observer Based on the Bouc–Wen Model for Smart Material-Actuated Systems," *Actuators*, vol. 13, no. 3, Mar. 2024, Art. no. 105, <https://doi.org/10.3390/act13030105>.
- [23] H. Zambare, A. Khoje, S. Patil, and A. Razban, "MR Damper Modeling Performance Comparison Including Hysteresis and Damper Optimization," *IEEE Access*, vol. 9, pp. 24560–24569, 2021, <https://doi.org/10.1109/ACCESS.2021.3057174>.